The EMBO Journal (2005) 24, 3770–3780 | © 2005 European Molecular Biology Organization | All Rights Reserved 0261-4189/05
www.embojournal.org

THE EMBO JOURNAL

KOPS: DNA motifs that control *E. coli* chromosome segregation by orienting the FtsK translocase

Sarah Bigot[1], Omar A Saleh[2], Christian Lesterlin[1], Carine Pages[1], Meriem El Karoui[3], Cynthia Dennis[4], Mikhail Grigoriev[4], Jean-François Allemand[2,5], François-Xavier Barre[1,*] and François Cornet[1,*]

[1]LMGM, CNRS, 118, route de Narbonne, Toulouse, France, [2]LPS, ENS, Paris, France, [3]URLGA, INRA, Jouy-en Josas, France, [4]LBME, CNRS, Toulouse, France and [5]Laboratoire Pasteur, departement de chimie, Paris, France

Bacterial chromosomes are organized in replichores of opposite sequence polarity. This conserved feature suggests a role in chromosome dynamics. Indeed, sequence polarity controls resolution of chromosome dimers in *Escherichia coli*. Chromosome dimers form by homologous recombination between sister chromosomes. They are resolved by the combined action of two tyrosine recombinases, XerC and XerD, acting at a specific chromosomal site, *dif*, and a DNA translocase, FtsK, which is anchored at the division septum and sorts chromosomal DNA to daughter cells. Evidences suggest that DNA motifs oriented from the replication origin towards *dif* provide FtsK with the necessary information to faithfully distribute chromosomal DNA to either side of the septum, thereby bringing the *dif* sites together at the end of this process. However, the nature of the DNA motifs acting as FtsK orienting polar sequences (KOPS) was unknown. Using genetics, bioinformatics and biochemistry, we have identified a family of DNA motifs in the *E. coli* chromosome with KOPS activity.

The EMBO Journal (2005) **24,** 3770–3780. doi:10.1038/sj.emboj.7600835; Published online 6 October 2005
Subject Categories: genome stability & dynamics; microbiology & pathogens
Keywords: chromosome segregation; FtsK translocase; replichores

Introduction

DNA translocases actively mobilize duplex DNA in a variety of cellular processes including DNA transfer between cells or cell compartments, DNA replication and segregation. In bacteria, members of the FtsK/SpoIIIE family of DNA translocases act during cell division to pump chromosomes out of division septa, thereby accurately sorting DNA to the correct side of the septum (Errington *et al*, 2001; Aussel *et al*, 2002). DNA trapping in a closing septum may result from a variety of abnormal chromosome processing events (i.e. replication, postreplicative restructuring or segregation failures). In two cases, however, DNA sorting by septum-associated translocases is recognized as a normal step of chromosome segregation. Sporulation of *Bacillus subtilis* involves chromosome trapping in an asymmetric septum followed by SpoIIIE-mediated translocation of the chromosome into the prespore (Errington *et al*, 2001). In *Escherichia coli*, FtsK serves to sort chromosomal DNA at cell division during resolution of chromosome dimers (Lesterlin *et al*, 2004). Chromosome dimers form by homologous recombination between circular sister chromosomes. Their resolution involves two tyrosine recombinases, XerC and XerD, acting at a specific 28 bp site located in the replication terminus, *dif*. FtsK plays two genetically separable roles in dimer resolution (Capiaux *et al*, 2002; Yates *et al*, 2003; Bigot *et al*, 2004; Massey *et al*, 2004). At the time of division, FtsK mobilizes the DNA stretches that cross the septum to bring the two *dif* sites together (Corre and Louarn, 2002; Bigot *et al*, 2004). It then specifically interacts with the XerCD/*dif* complex to induce recombination, allowing resolution of the dimer (Aussel *et al*, 2002; Yates *et al*, 2003; Massey *et al*, 2004).

The direction of translocation through the septum is crucial for the accurate sorting of chromosomal DNA, both in *B. subtilis* sporulation and in *E. coli* chromosome dimer resolution (CDR). Anchoring of SpoIIIE on a specific side of the asymmetric sporulation septum can impose translocation directionality in *B. subtilis* (Sharp and Pogliano, 2002), but no such asymmetry exists in the *E. coli* cell division septum. It has been proposed that the DNA tensions generated by condensation of the sister chromosomes may impose directionality to FtsK translocation (Saleh *et al*, 2004). However, several sets of data indicate that the direction of translocation is controlled by the translocated DNA itself. *In vivo* experiments revealed that dimer resolution depends on the orientation of the sequences flanking *dif* (Cornet *et al*, 1996; Kuempel *et al*, 1996; Perals *et al*, 2000). Indeed, *dif* needs to lie at the junction of the two chromosome arms running from the replication origin to *dif*, the replichores, to be active in CDR (Lesterlin *et al*, 2005). Insertion of the bacteriophage λ in the vicinity of *dif* inhibits dimer resolution in one orientation, which gives rise to a phenomenon of local homologous hyper-recombination (Corre *et al*, 2000). The orientation that inhibits dimer resolution switches at *dif*, suggesting that the λ genome displays the same polarization signals as the replichores. The hyper-recombination phenomenon becomes independent of prophage orientation in mutants lacking the translocation activity of FtsK, further suggesting that replichore polarity controls the direction

*Corresponding authors. F-X Barre, CGM, CNRS, Avenue de la Terrasse, 91198 Gif-sur-Yvette, France. Tel.: +33 169 82 32 24; Fax: +33 169 82 31 60; E-mail: Francois-Xavier.Barre@cgm.cnrs-gif.fr or F Cornet, LMGM, CNRS, 118, route de Narbonne, 31062 Toulouse Cedex, France. Tel.: +33 561 335 986; Fax: +33 561 335 886; E-mail: cornet@ibcg.biotoul.fr

Received: 8 June 2005; accepted: 14 September 2005; published online: 6 October 2005

of FtsK translocation (Corre and Louarn, 2002; Bigot *et al*, 2004). *In vitro*, a purified truncated derivative of FtsK, $FtsK_{50C}$, can translocate on all pieces of DNA tested so far (Aussel *et al*, 2002; Massey *et al*, 2004; Saleh *et al*, 2004; Pease *et al*, 2005). A first attempt, using a single molecule approach with a chromosome fragment shown to affect dimer resolution when inverted, failed to reveal an effect of sequence orientation (Saleh *et al*, 2004). This suggested that polarization reading by FtsK is either indirect or highly stochastic, preventing the detection of its effect under these conditions. However, the observation, by light microscopy, that large aggregates of $FtsK_{50C}$ translocate directionally on bacteriophage λ DNA and on chromosomal DNA of the *dif* region strongly suggested that polarization is directly read by FtsK (Pease *et al*, 2005).

The nature of the chromosomal elements that function as FtsK orienting polar sequences (KOPS) is a long-standing question. A number of DNA motifs display a biased orientation following the origin to *dif* axis (Blattner *et al*, 1997). Among these, short degenerate motifs, termed RAG, have been proposed as good candidates based on their highly biased orientation (Lobry and Louarn, 2003). However, previous attempts to show that the RAG motif controls FtsK activity or to localize other active elements were unfruitful (Perals *et al*, 2000; Massey *et al*, 2004; Saleh *et al*, 2004). Here, we used a functional approach to identify motifs in the *E. coli* genome that inhibit CDR in an orientation-dependent manner. Compilation of functional and predictive data shows that they are a family of motifs, 5′-GGGNAGGG-3′, displaying a highly biased orientation and over-represented on the whole chromosome. *In vitro,* these motifs display KOPS activity: they inhibit Xer recombination activation by FtsK in an orientation-dependent manner; they stop FtsK from dissociating branched DNA structures depending on their orientation; additionally, single molecule data suggest that they block FtsK translocation. Lastly, their effect on FtsK translocation is stochastic; the presence of two or three motifs is required to observe a strong effect.

Results

Short DNA sequences inhibit chromosome dimer resolution

The efficiency of CDR can be assessed using a simple coculture assay. This assay measures the selective growth advantage of a strain compared with a *dif*-deleted strain in which 15% of the cells carry an unresolved dimer and thus fail to produce a viable progeny (Materials and methods; Perals *et al*, 2000). CDR is inhibited by *dif* displacement or by inversion of DNA segments surrounding *dif* (Cornet *et al*, 1996; Perals *et al*, 2000). In both cases, the extent of the inhibition depends on the length of the improperly oriented DNA that flanks *dif* and is only detectable if the DNA fragment is larger than 6 kb (Lesterlin *et al*, 2005; F Cornet, unpublished results). However, CDR appears more sensitive to improperly oriented DNA when *dif* is replaced by *psi*, a plasmid-borne target for XerCD (Cornet *et al*, 1994). CDR at *psi* is less efficient than at *dif* but strictly depends on FtsK (Capiaux *et al*, 2002; Figure 1B, line 2). Inserting *psi* 8869 bp away from the normal *dif* position led to a complete inhibition of CDR (*zdd355* position; Figure 1B, line 3), whereas about 90% of the dimers are resolved when *dif* is inserted at this same position (Perals *et al*, 2000). This observation prompted us to locate CDR-inhibiting motifs in strains in which *dif* has been deleted and *psi* inserted at different positions.

A set of strains was constructed that carry *psi* at the *zdd355* position and progressive deletions of the 8869 bp fragment, following the procedure described in Figure 1A (see also Materials and methods). As expected, deletion of the entire 8869 bp fragment restored CDR (Figure 1B, line 4). Two significant transitions in CDR activity were found. One occurs along a 30 bp fragment (fragment I) located 2970 bp away from the normal *dif* position (Figure 1B, compare line 9 with 10) and the other occurs along a 1120 bp fragment (fragment II) located 3370 bp away from *dif* (Figure 1B, compare line 6 with 7). These two fragments were thus each inferred to carry at least one CDR-inhibiting motif.

CDR-inhibiting sequences are specific and degenerate motifs that act in an orientation-dependent manner

To obtain further insights into the nature of the CDR-inhibiting motifs, the CDR-inhibiting fragment I (Figure 1B) was inverted with respect to *psi*. The strain constructed is isogenic to strain no. 9 in Figure 1 except for the inverted sequence. Thus, a fully active motif should yield a CDR of ∼45% compared to ∼65% if its CDR-inhibiting activity is eliminated. As expected, inversion of fragment I eliminated CDR-inhibiting activity (Table I, line 2), showing that the CDR-inhibiting motif functions in an orientation-dependent manner. Comparison of the CDR-inhibiting fragments I and II (Figure 1B) showed that their longest common sequence is an 8 bp motif, 5′-GGGAAGGG-3′. Inversion of a 12 bp fragment encompassing this motif in fragment I eliminated CDR-inhibiting activity (Table I, line 3), further suggesting that GGGAAGGG is the CDR-inhibiting motif carried by both CDR-inhibiting fragments.

Figure 2A shows the distribution of the GGGAAGGG motif in the *dif* region (line 4) together with the location of the fragments previously shown to inhibit CDR when inverted (line 3; Perals *et al*, 2000; Lesterlin *et al*, 2005). As expected, the GGGAAGGG motifs are strictly oriented towards *dif*. However, this motif is absent from two of the four fragments that inhibit CDR when inverted (fragments B and D), suggesting that it does not, alone, account for CDR-inhibiting activity. Based on the assumption that CDR-inhibiting motifs must be frequent and highly skewed in the whole *E. coli* chromosome (Perals *et al*, 2000; Lesterlin *et al*, 2005), we analysed the skew and frequency of occurrence of all 6, 7 and 8 bp motifs present in CDR-inhibiting fragment I, allowing a single base degeneracy. To assess the significance of the skews, a statistical test was developed that takes into account the asymmetric base composition of leading and lagging strands of the chromosome (Materials and methods). Table II reports the data obtained for motifs with significant skews (S-skew > 3.84, meaning that the skew is significant with a 95% confidence, Materials and methods). Strikingly, the most skewed motifs contain the GNAG motif and are contained in the GGGNAGGG motif. This motif is strictly oriented towards *dif* in the *dif* region (Figure 2A, line 5) and strongly skewed along the replichores in the whole chromosome (Figure 2B). Moreover, its distribution is in accord with previous data obtained from chromosome inversion experiments (Figure 2A). This motif is also largely over-represented

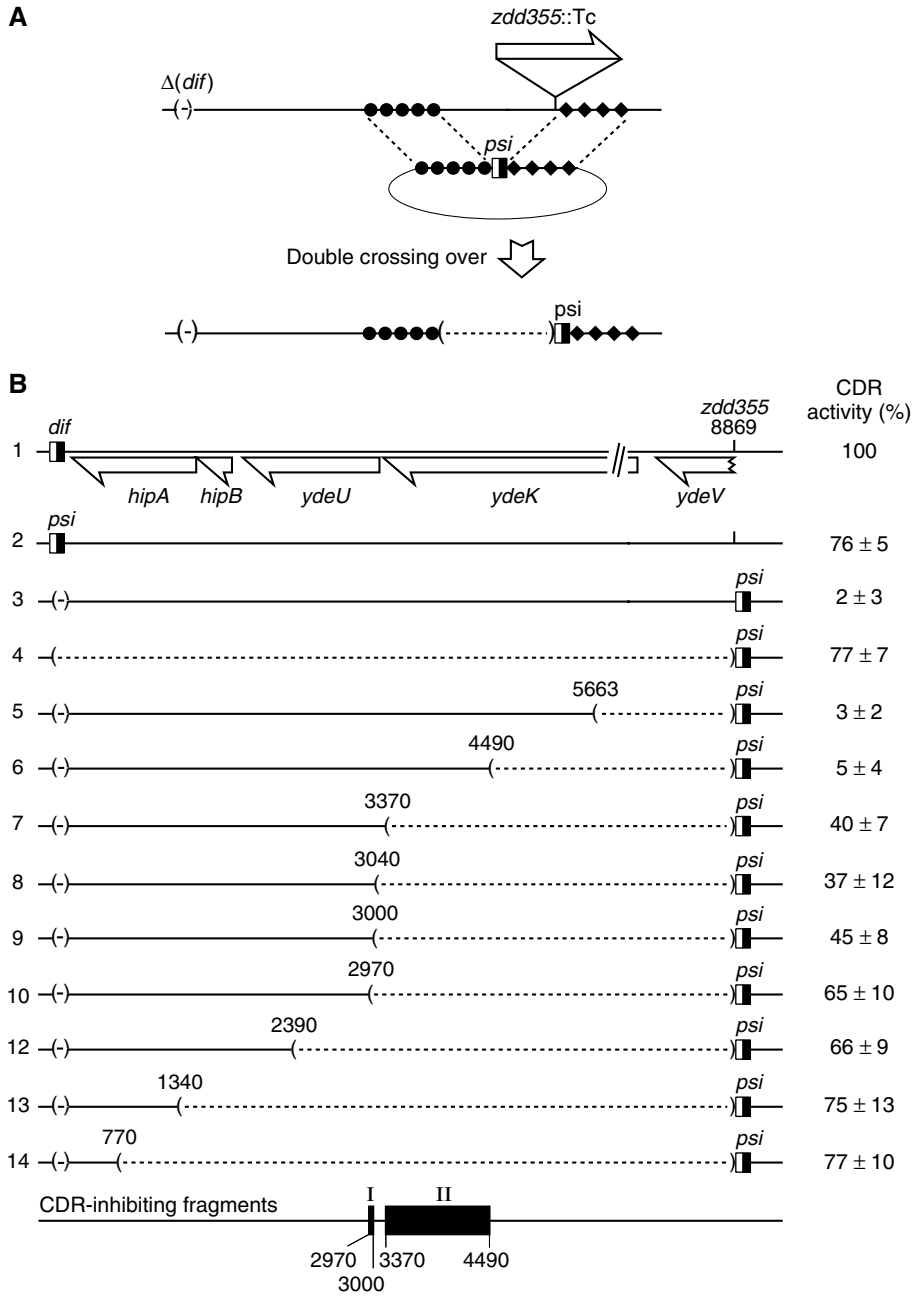

Figure 1 Localization of sequences controlling dimer resolution. (**A**) Strategy used for strain construction. Strain FC53 (top line) carries a 58 bp *dif* deletion and a tetracycline resistance determinant (Tc) inserted at position *zdd355* (Materials and methods). Relevant chromosome fragments, indicated by black circles and black diamonds,, were cloned on each side of the *psi* site into a transgenesis vector and the resulting constructs were installed on the chromosome, screening for tetracycline-sensitive clones at the end of the procedure (Materials and methods). The resulting strains carry the *psi* site in place of a deleted fragment at the *zdd355* edge of the *dif-zdd355* fragment (bottom line). Deleted fragments are shown as dotted lines in parentheses. (**B**) Line 1 shows a map of the *dif-zdd355* region. The arrows represent genes and the black and white square the indicated recombination site, *dif* or *psi*. Coordinates are in bp from the *dif* position. The fragments inferred to have CDR-inhibiting activity from these experiments are shown as black bars on the last line and named fragments I and II. Line 2: *dif* has been replaced by the *psi* site (redrawn from Capiaux *et al*, 2002). Line 3: *dif* has been deleted and *psi* inserted at the *zdd355* position. Lines 4–14: *psi* has been inserted in place of the deletions of the indicated fragments. Deleted fragments are shown as dotted lines in parentheses. CDR activities of the strains carrying the different constructs are given on the left expressed in % of full resolution activity (100% in a wild-type strain and 0% in a *dif*-deleted strain) with standard deviations. They were measured using the coculture assay (Materials and methods). Each point is the mean of three independent experiments except for lines 9 and 10 for which the mean of five experiments is reported.

(S-occ > 7, corresponding to a probability of random occurrence $<10^{-12}$), suggesting that it has been selected and maintained in the genome. The GGGNAGGG motif is thus the longest motif in accord with all available data and was thus used for further functional analysis.

The specificity and degeneracy of the CDR-inhibiting motif present in CDR-inhibiting fragment I was tested by mutation. Changing the central AA to CA conserved CDR-inhibiting activity (Table I, line 4), showing that CDR-inhibiting motifs are degenerate at least at this position. In contrast, changing

Table I Mutational analysis of the 30 bp sequence shown to contain a CDR-inhibiting motif

No.	Sequence (5′–3′)	CDR activity (%)
1	ACGCTGGCTAAAGGGAAGGGGAATGACGAG	45 ± 10
2	**CTCGTCATTCCCCTTCCCTTTAGCCAGCGT**	71 ± 5.6
3	ACGCTGGCTA**TCCCCTTCCCTT**ATGACGAG	70 ± 11
4	ACGCTGGCTAAAGGG**C**AGGGGAATGACGAG	37 ± 17
5	ACGCTGGCTAAAGGGA**T**GGGGAATGACGAG	67 ± 8.6
6	ACGCTGGCTAAA**GGGCAGGGCAGGGCAGGG**AATGACGAG	23 ± 7

CDR-inhibiting fragment I (positions 2970–3000 in Figure 1) is shown in line 1 with the GGGAAGGG motif common to CDR-inhibiting fragment II (positions 3370–4490 in Figure 1) underlined. The sequence is represented in opposite orientation with respect to the chromosome so that the GGGAAGGG motifs is 5′ to 3′ on the top strand. Constructions were inserted on the chromosome to yield strains isogenic to strain no. 9 in Figure 1 except for the mutations. Lines 2–6: changes with respect to the wt sequence are shown in bold; line 2: inversion of the entire 30 bp sequence; line 3: inversion of 12 bp containing the GGGAAGGG motif; lines 4 and 5: point mutations; line 6: replacement of the GGGAAGGG motif with three overlapping GGGCAGGG motifs. The dimer resolution (CDR) activities of the resulting strains were measured as in Figure 1 (mean of three independent experiments).

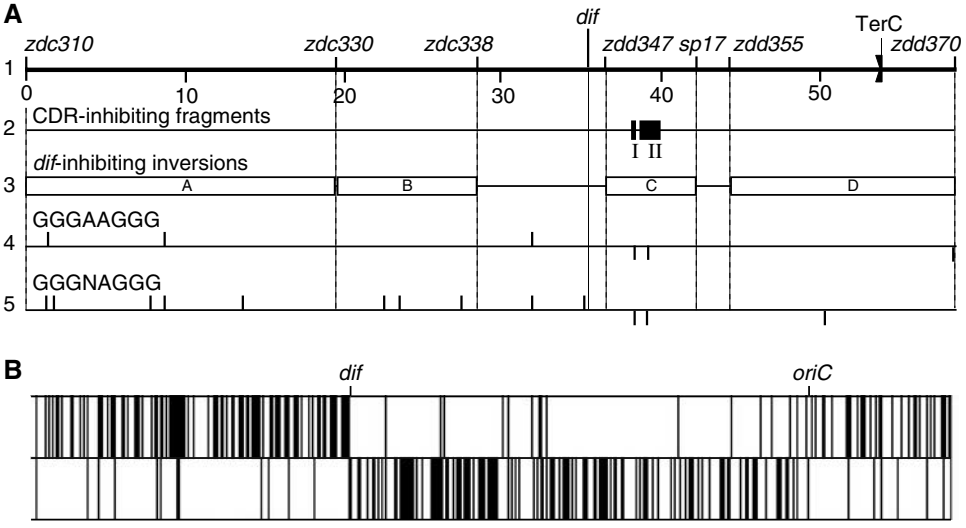

Figure 2 (**A**) Distribution of the candidate motifs on the chromosome. Line 1 is a map of the 58 502 bp chromosome region between positions *zdc310* and *zdd370* in which inversions decrease the efficiency of CDR (Perals *et al*, 2000; Lesterlin *et al*, 2005). Coordinates are in kb. The positions of the end points of previously reported inversions (the *zdc*, *zdd* and *sp17* positions) are shown together with the positions of *dif* and its closest replication terminator, TerC. Line 2 indicates the position of the two CDR-inhibiting fragments inferred from the experiment reported in Figure 1 (fragments I and II shown as black bars). Line 3 shows the fragments that inhibit *dif* activity when inverted (the A, B, C and D open bars; redrawn from Perals *et al*, 2000; lesterlin *et al*, 2005). Lines 4 and 5: distribution of the indicated motifs on the top (above the lines, 5′ to 3′ left to right) and bottom (below the lines, 5′ to 3′ right to left) strand. (**B**) Distribution of the GGGNAGGG motif on the entire chromosome. The positions of the replication origin, *oriC*, and *dif* are indicated. Each vertical bar represents a GGGNAGGG motif on the top (upper bar) or on the bottom (lower bar) strand.

the AA to AT eliminated CDR-inhibiting activity (Table I, line 5), showing that CDR-inhibiting motifs are specific sequences.

GGGNAGGG motifs only partially inhibit CDR. A single motif in nonpermissive orientation yields a decrease of 20–30% in CDR activity, whereas two motifs yield a more severe decrease (Figure 1B and Table I). To confirm this observation, the single motif present in CDR-inhibiting fragment I was replaced by three overlapping GGGCAGGG motifs. As expected, the three overlapping motifs have a significantly higher effect than a single motif (Table I, line 6).

GGGNAGGG motifs control Xer recombination in vitro

To demonstrate that GGGNAGGG motifs have KOPS activity, we first tested their effect on FtsK-dependent Xer recombination *in vitro*. The assay detects recombination between a short labelled 34 bp *dif*-containing DNA fragment and a longer DNA fragment carrying about 260 bp on one side of *dif* in the presence of purified XerC, XerD and a purified truncated version of FtsK, $FtsK_{50C}$ (Aussel *et al*, 2002; Massey *et al*, 2004; Figure 3A). Loading of $FtsK_{50C}$ on duplex DNA adjacent to *dif* is required for interaction with XerCD/*dif* and activation of recombination. Efficient loading requires at least 180 bp of duplex DNA (Yates *et al*, 2003; Massey *et al*, 2004). Thus, insertion of KOPS between *dif* and the 260 bp DNA duplex could prevent $FtsK_{50C}$ from reaching XerCD/*dif* and thereby affect the efficiency of recombination. The DNA motifs to be tested were inserted in both orientations on the long fragment (Figure 3A) and the efficiency of recombination obtained for both orientations were compared (Figure 3B). Constructs carrying the CDR-inhibiting fragment I (Table I, line 1) in nonpermissive orientation recombined about 50% less efficiently than the permissive orientation, strongly suggesting that this sequence has KOPS activity and

Table II Skew and frequency of occurrence on the chromosome of degenerated 6–8 bp motifs found in CDR-inhibiting fragment I

Size (bp)	Motif	Skew	S-skew	Occ (L/l)	S-occ
6	GANGGG	0.6	4.42	3547/2364	1.76
	AGGGNA	0.61	7.86	3385/2182	3.33
	ACGTNG	0.53	7.94	4008/3578	1.8
	AGGNGA	0.57	8.37	4647/3440	3.87
	GGGNAA	0.55	9.24	5765/4762	5.29
	GGGNAG	0.62	23.52	3840/2374	−0.57
	GNAGGG	0.67	54.25	3747/1836	6.73
7	AGGGNAA	0.57	4.86	1259/963	2.72
	TNAAGGG	0.58	5.22	697/506	−6.51
	GAANGGG	0.63	5.52	1132/677	8.28
	GGNAAGG	0.58	5.91	1049/749	1.19
	GGANGGG	0.67	11.4	814/410	4.45
	GNAAGGG	0.66	13.77	1081/545	7.65
	AGGGNAG	0.72	20.81	804/305	0.14
	GGGNAGG	0.72	24.2	962/371	5.55
	GGNAGGG	0.75	24.44	1106/362	7.47
8	GNAAGGGG	0.76	3.95	288/89	2.21
	GNGAAGGG	0.72	4.48	333/130	3.41
	GNAGGGGA	0.8	5	326/84	3.76
	GGNAGGGG	0.83	5.47	287/57	2.34
	GGGNAGGG	0.91	14.49	335/33	7.18

All 6–8 bp motifs contained in CDR-inhibiting fragment I (Figure 1B) were analysed for their skew and frequency on the *E. coli* chromosome (Materials and methods). Significantly skewed motifs are presented (S-skew >3.84). Skew: proportion of motifs on the leading strand divided by the total number; S-skew: statistical significance of the skew (see Materials and methods); Occ (L/l): number of occurrences on the leading (L) and lagging (l) strands of the chromosome; S-occ: statistical significance of the number of occurrences on the leading strand. S-occ >5 indicates that the motif is highly over-represented (probability of random occurrence is $<10^{-7}$). Negative S-occ indicates that the motif is under-represented.

that KOPS are directly recognized by FtsK (Figure 3B, panel 1). Insertion of a single GGGCAGGG motif had the same effect (Figure 3B, panel 2), showing that this motif alone contains the information required to inhibit Xer recombination.

Since CDR-inhibiting motifs have partial but cumulative effects *in vivo* (Figure 1B and Table I), we tested the effect of several consecutive motifs on Xer recombination. Three overlapping GGGCAGGG motifs had cumulative effects yielding an ~10-fold ratio in recombination efficiency between the permissive and nonpermissive orientation (Figure 3B, panel 4). Two consecutive motifs separated by 6 bp also had cumulative effects (Figure 3B, panel 3). This suggests that the effect of the GGGNAGGG motifs is stochastic; the presence of several motifs is required to observe a strong effect *in vivo* and *in vitro*. This is reminiscent of the way Chi motifs affect the activity of the RecBCD helicase *in vitro* (Dohoney and Gelles, 2001; Spies *et al*, 2003).

The three overlapping motifs were then used to check for the sequence specificity of the inhibiting motif in the recombination assay. As expected, the three overlapping motifs with an AT central dinucleotide did not provoke any significant inhibition in the nonpermissive orientation (Figure 3B, panel 6). Lastly, a shuffled poly-purine tract, with a composition equivalent to the three overlapping GGGCAGGG motifs, did not inhibit recombination, further indicating that the inhibiting effect is sequence specific rather than due to the GC bias and/or purine richness of the motif (Figure 3B, panel 5).

GGGNAGGG motifs control FtsK translocation

To assess whether the GGGNAGGG motif affects the activity of FtsK independently from Xer recombination activation, we developed an assay based on the observation that translocases can dissociate branched DNA structures as shown for the DnaB helicase (Kaplan and O'Donnell, 2004). A T-shaped substrate was designed, consisting of a DNA duplex with 20 noncomplementary bases at one extremity, annealed to a labelled 40-mer oligonucleotide (Figure 4A; Materials and methods). As shown in Figure 4B, $FtsK_{50C}$ can displace the labelled strand of this substrate. This activity depends on ATP hydrolysis and on the length of the duplex DNA (not shown). At least 180 bp of duplex DNA is required, which correlates with the minimum DNA length required in the recombination assay (Massey *et al*, 2004). We thus conclude that the rate of displacement of the labelled strand reflects the efficiency of $FtsK_{50C}$ translocation.

The three overlapping GGGCAGGG motifs (Figure 3B, panel 4) were inserted in both orientations next to the T-shaped end of the substrate (Figure 4A) and their effect on displacement of the labelled strand was observed in kinetic experiments (Figure 4B and C). As expected, the motifs strongly inhibited strand displacement in an orientation-dependent manner. Thus, the GGGNAGGG motifs control FtsK translocation on duplex DNA in an orientation-dependent manner, showing that they have KOPS activity. Interestingly, we did not observe a significant effect of a single GGGNAGGG motif using the T-dissociation assay (not shown), further suggesting that KOPS recognition by FtsK is stochastic.

KOPS block DNA translocation of a single FtsK motor

$FtsK_{50C}$ can form DNA loops *in vitro* (Aussel *et al*, 2002; Ip *et al*, 2003). This property has been used to monitor $FtsK_{50C}$ translocation using a magnetic tweezer-based experimental design (Saleh *et al*, 2004). In this system, a single nicked DNA molecule that tethers a magnetic bead to a glass capillary

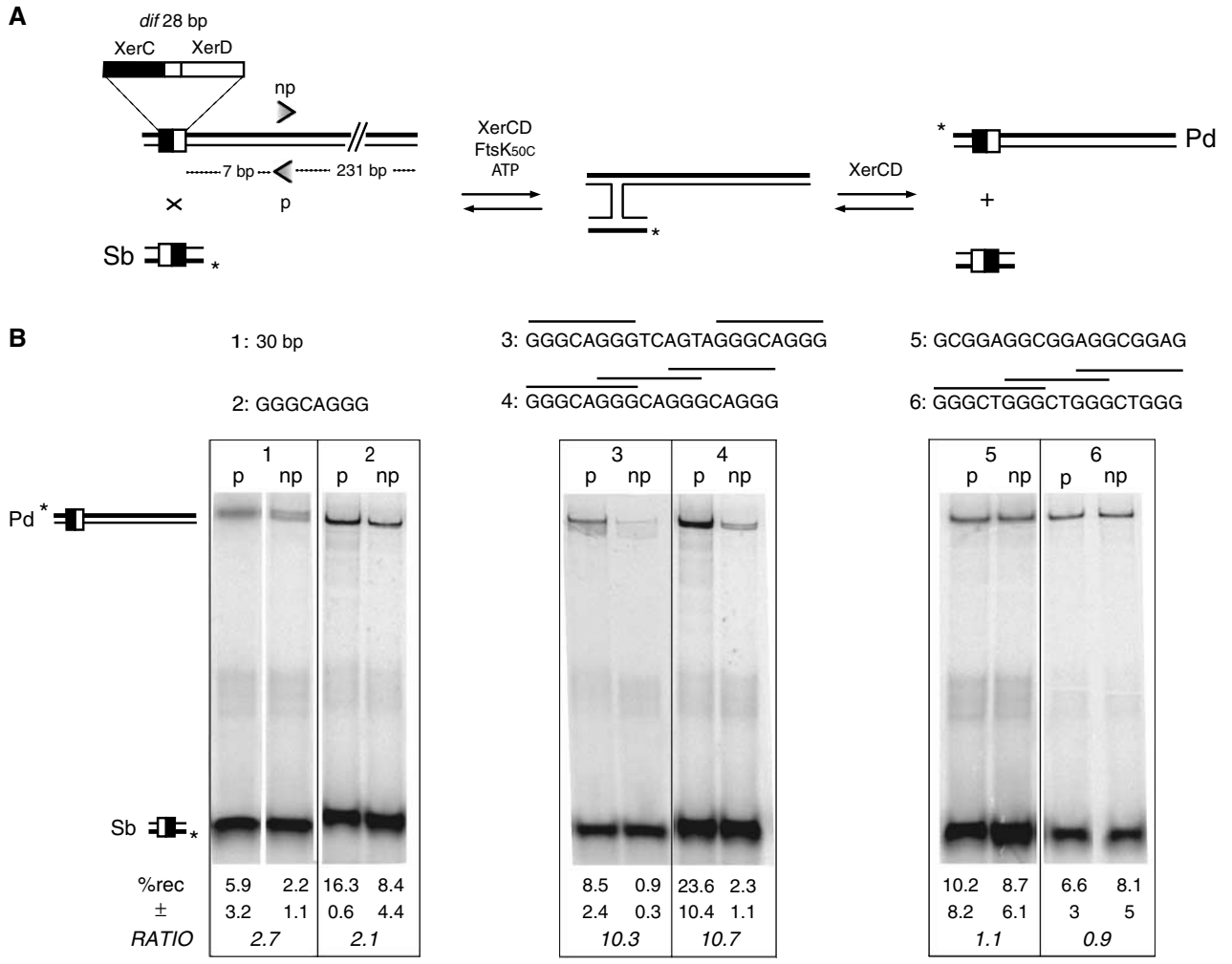

Figure 3 Effect of GGGNAGGG motifs on FtsK-dependent Xer recombination. (**A**) System used. The black and white square represents *dif* and the arrowhead a GGGNAGGG motif (np: nonpermissive orientation; p: permissive orientation). The star indicates the labelled extremity (the 5′ end of the strand cleaved by XerC on the short substrate). Sb and Pd indicate the two forms detected on the gels and used for quantification (substrate and product, respectively). Exchange of a first pair of strands is catalysed by XerD in the presence of XerC and $FtsK_{50C}$ and leads to a Holliday junction-containing intermediate. Exchange of the second pair of strands is catalysed by XerC and does not require FtsK. (**B**) Effect of the indicated motifs on recombination. The form corresponding to the two bands is drawn on the left (Sb and Pd). p: permissive orientation of the motif; np: nonpermissive orientation. The percentage of recombinant product (ratio of Pd DNA over total DNA (Sb + Pd)) is given below each lane (%rec, mean of three independent experiments with standard deviation (±)). Below each panel, *RATIO* indicates the ratio of the %rec obtained in permissive (p) and nonpermissive (np) orientation (mean of the ratios calculated for each independent experiment). Panel 1: the motif inserted is the 30 bp sequence shown in Table I, line 1. Panels 2–6: the sequences of the inserted motifs are shown. Panel 2: one GGGCAGGG motif. Panel 3: two GGGCAGGG motifs separated by 6 bp. Panel 4: three overlapping motifs. Panel 5: shuffled sequence. Panel 6: three overlapping GGGCTGGG motifs.

tube is stretched with a constant force using external magnets (Figure 5A) (Strick *et al*, 1996). Loop extrusion by $FtsK_{50C}$ brings the bead towards the glass surface (Figure 5A). $FtsK_{50C}$ can also switch direction, shortening the DNA loop and allowing the bead to rise up (Saleh *et al*, 2004). Thus, tracking the height of the bead allows monitoring of $FtsK_{50C}$ translocation in real time. Care was taken to work in conditions in which translocation events are clearly separated in time to ensure that the activity of a single FtsK motor was monitored (Materials and methods; Saleh *et al*, 2004).

At low stretching forces (<5 pN), translocation events in which the bead is brought completely down to the glass surface and then brought back to full extension at a similar speed are frequently observed (Saleh *et al*, 2004). We reasoned that if KOPS have a strong effect on FtsK translocation, their presence on the DNA substrate should abolish or modify these events. In a previous report, we did not observe such an effect when using a 14 kb *E. coli* chromosomal fragment shown to be polarized *in vivo* (Saleh *et al*, 2004). However, we now know that this fragment contains only one GGGNAGGG motif. The absence of detectable activity may thus be due to the moderate activity of a single motif, as observed in the Xer recombination and T-shaped end assays. We constructed a 10.5 kb DNA molecule with three overlapping GGGCAGGG motifs (Figure 3B, panel 4) inserted at 3.2 kb from the bead and pointing towards the bead (Figure 5B). Using this molecule, the majority of translocation events now terminated or switched direction at the position where the motifs had been inserted (Figure 5C). Equivalent results were obtained with the three overlapping

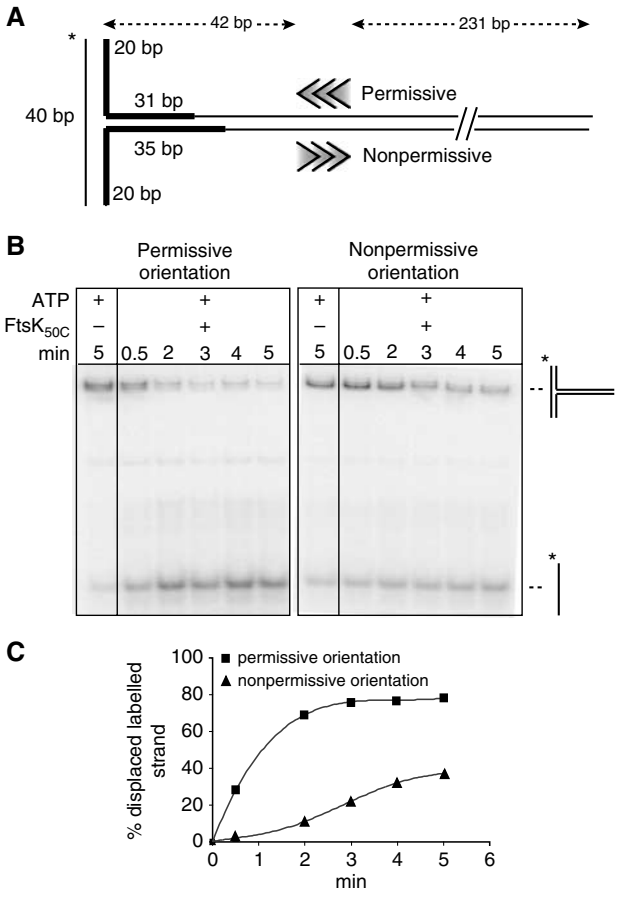

Figure 4 GGGNAGGG motifs inhibit dissociation of branched DNA structures by FtsK in a specific orientation. (**A**) Schematic representing the T-shaped substrate used (see Materials and methods). Distances in bp are indicated. The two 51- and 55-mer oligonucleotides with 20 bp noncomplementary extremities are shown in bold. These are ligated with a 260 bp DNA fragment allowing the loading of $FtsK_{50C}$. The 40-mer oligonucleotide complementary to the forked structure is labelled (*). The concatenated arrowheads indicate the position of the three overlapping GGGCAGGG motifs (same as in Figure 3, panel 4) inserted in permissive and nonpermissive orientation. (**B**) Kinetics of T-shaped substrate dissociation by FtsK. Control lanes with no FtsK are shown on the left of each gel. The forms corresponding to the two bands are shown on the right. (**C**) Quantitative analysis of the amount of dissociated oligonucleotide due to $FtsK_{50C}$ activity. The amount of displaced oligonucleotide in the presence of $FtsK_{50C}$ was corrected by subtracting the percentage of displacement obtained in the absence of $FtsK_{50C}$ after 5 min. The value obtained was used to calculate the percentage of $FtsK_{50C}$-dependent displacement (% displaced label strand axis) and plotted as a function of time.

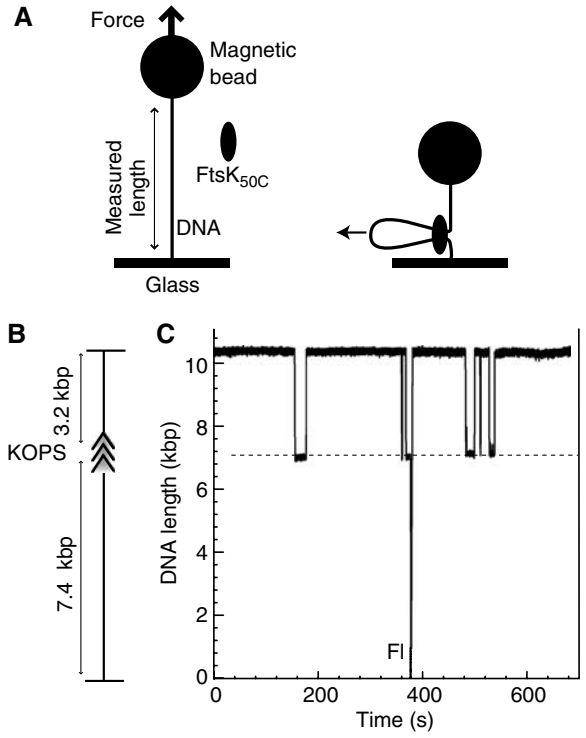

Figure 5 GGGNAGGG motifs block FtsK translocation at the single molecule level. (**A**) Schematic representation of the measurement apparatus and of the decrease of DNA extension due to loop formation by $FtsK_{50C}$ (see Materials and methods). (**B**) Schematic of the 10.5 kb DNA substrate used, with position and orientation of the three overlapping GGGCAGGG motifs (the three concatenated arrowheads) shown. Distances in kbp are indicated. (**C**) Typical translocation events on the DNA substrate shown in panel B. The experiment was carried out at 5 mM ATP, pulling on the bead at 1 pN. The position of the bead, expressed in kbp equivalent, is plotted as a function of time. Data quoted in units of base pairs have been corrected for the difference between the measured DNA extension and the true contour length by applying the worm-like chain model for DNA elasticity (Bouchiat *et al*, 1999). The dotted line indicates the position of the motifs. Fl: an example of full-length translocation event.

motifs at the centre of the DNA substrate or when they pointed towards the glass surface rather than the bead (data not shown). These results strongly suggest that the GGGNAGGG motif blocks DNA translocation by FtsK.

Discussion

E. coli chromosome segregation is controlled by short degenerate DNA motifs that orient FtsK translocation

We report here the identification of a family of DNA motifs in the *E. coli* genome that control the direction of FtsK translocation, and thereby its capacity to reach the *dif* sites and activate CDR. These motifs inhibit CDR when inserted in the vicinity of the resolution site in their nonpermissive orientation (Figure 1 and Table I). This effect correlates with an inhibition of Xer recombination in an *in vitro* assay that requires the loading of FtsK on duplex DNA (Figure 3). Finally, these motifs control translocation of FtsK in two assays independent of Xer recombination, one using the capacity of FtsK to dissociate branched DNA structures and the other its capacity to create DNA loops when translocating on DNA. Taken together, these results show that these motifs function as KOPS.

The nature of KOPS

The GGGAAGGG motif, common to the two CDR-inhibiting fragments located *in vivo* (Figure 1B), does not account alone for KOPS activity in the *dif* region (Figure 2A). A search for the most skewed motifs allowing 1 bp degeneracy points to the GGGNAGGG consensus. In favour of this consensus, both GGGAAGGG and GGGCAGGG motifs have KOPS activity *in vitro*, the distribution and orientation of the GGGNAGGG motif fits with functional data (Figure 2A) and it is highly skewed along the replichores on the whole chromosome (Figure 2B). However, shorter or more degenerate motifs

may also have KOPS activity. In this view, examination of the distribution and orientation in the *dif* region of the 6 and 7 bp motifs contained in the GGGNAGGG motif suggests that it may be degenerate for its first two bases but not for the last two. For instance, the GGNAGGG motif would fit the functional data as well as the GGGNAGGG motif (not shown). In addition, the GGGNAGGG motif is present only twice, once in each orientation, in the bacteriophage λ genome, which displays a strong KOPS activity (Corre *et al*, 2000). A GNGNAGGG consensus would better explain the data from λ insertions. Interestingly, a GCGAAGGG motif is present at 2305 bp to the left of *dif* and may account for a moderate decrease in CDR activity when present in nonpermissive orientation (compare line 12 with 13 in Figure 1). Further studies will be required to refine the KOPS consensus. Motifs smaller or more degenerate than GGGNAGGG could have a weaker effect on FtsK translocation, making their activity difficult to detect when they are not sequentially repeated.

The GGGNAGGG motif, particularly if degenerate for its first two bases, overlaps the RAG motif (5′-RGNAGGGS-3′; R = A or G, S = G or C) previously proposed to play an orienting role in chromosome processing based on its high skew (Lobry and Louarn, 2003). However, RAG does not stand as a good consensus for KOPS since the CDR-inhibiting fragment II (Figure 1B and 2A) is devoid of RAG. On the other hand, a fragment containing three RAG, GGCAGGGG, AGCAGGGC and AGCAGGGG (a 4.5-kb-long fragment directly right from the *zdd355* position), has no effect on CDR when placed in nonpermissive orientation next to *dif* (Cornet *et al*, 1996) or next to *psi* (F Cornet, unpublished). Thus, even if some RAG motifs may have KOPS activity, the KOPS and RAG consensus are different.

The effect of KOPS is stochastic

The necessity to alter more than 6 kb of chromosomal DNA around *dif* to affect CDR *in vivo* suggested that KOPS do not have an 'all or nothing' effect but a moderate activity. This prompted us to lower the activity of the CDR system, by replacing *dif* by *psi*, to detect the effect of a single KOPS. The 28 bp *psi* site used diverges from *dif* by a few base pairs, which lowers its capacity to enter the FtsK-dependent pathway of Xer recombination, the only one allowing CDR (Capiaux *et al*, 2002). This certainly results from a preferred conformation of the XerCD/*psi* complex inappropriate to FtsK-dependent recombination (Aussel *et al*, 2002; Capiaux *et al*, 2002; Lesterlin *et al*, 2004). The fact that XerCD/*psi* system is more sensitive than XerCD/*dif* to inverted KOPS may be a consequence of the spatio-temporal control of CDR (Lesterlin *et al*, 2004). In particular, unresolved dimers do not block septation and are guillotined (Hendricks *et al*, 2000). The resolution system may thus have a limited time to resolve a dimer, corresponding to a fixed mean number of attempts. This may not be sufficient in all cases with the *psi* site if the majority of events fail due to improper conformation of the recombination complex.

Consistent with the moderate activity of the KOPS *in vivo*, a single KOPS does not completely block Xer recombination activation by $FtsK_{50C}$ *in vitro* (Figure 3B). In both cases, the inhibitory effect could be increased by placing several consecutive KOPS in nonpermissive orientation (Table I and Figure 3B). Consistently, we had to use several consecutive KOPS to observe a significant effect in two independent translocation assays, one making use of the ability of $FtsK_{50C}$ to open branched DNA structures (Figure 4) and the other monitoring translocation of single $FtsK_{50C}$ complexes (Figure 5). These data are most easily explained if KOPS recognition by FtsK is stochastic: during translocation, FtsK can be stopped or not stochastically by a single KOPS and the chances of affecting translocation increases with their number. Why then is translocation of large aggregates of $FtsK_{50C}$ strictly oriented on *E. coli* or bacteriophage λ DNA as demonstrated by their direct observation by light microscopy (Pease *et al*, 2005)? These aggregates were observed at an $FtsK_{50C}$ concentration of about 150 nM. In our system, at concentrations higher than 15 nM, translocation events become so frequent that they cannot be attributed to single $FtsK_{50C}$ complexes (see Supplementary Figure and Materials and methods). We therefore speculate that several motors are active at the same time in the large $FtsK_{50C}$ aggregates observed by Pease and co-workers. This may increase the chance that a single KOPS is recognized in the same manner, as increasing the number of KOPS increases the chance of their recognition by a single motor.

KOPS are highly skewed and over-represented in the E. coli genome

The stochastic effect of KOPS is reminiscent of the way Chi sites affect the activity of the RecBCD exonuclease in an oriented and stochastic manner (Taylor *et al*, 1985; Dixon and Kowalczykowski, 1995; Dohoney and Gelles, 2001; Spies *et al*, 2003). This mode of control of DNA traffic contrasts with the way Ter sites bound by the Tus protein block replication forks (Hill and Marians, 1990; Hill, 1992; Kamada *et al*, 1996). Interestingly, the stochastic effect of KOPS and Chi sites is accompanied by a high, but not total, skew and an over-representation of these motifs on the chromosome (Table II; El Karoui *et al*, 1999). Strikingly, the GGGNAGGG motif is the second most skewed, the first being a degenerated Chi site. It is also the 46th most represented 8 bp motif with a single degeneracy on the chromosome (not shown).

An absence of absolute skew, combined with a stochastic activity, may be required to process rare events independent of CDR. For instance, DNA loops lacking the replichore junction may be trapped in the septum. Processing these loops would require translocation of the entire chromosome if the direction of FtsK translocation was absolute, which seems unlikely. In such cases, the moderate effect of KOPS may allow the DNA tension generated by segregation and condensation of the sister chromosomes to drive processing of the loops, as previously proposed (Saleh *et al*, 2004).

Why should KOPS be so numerous? The mean processivity of the FtsK translocation complex was found to be on the order of 22 kb (Saleh *et al*, 2004). This suggests that during translocation of DNA through the septum, a new pump might need to be loaded as frequently as every 22 kb. The mean frequency of occurrence of the GGGNAGGG motif on the chromosome is high, due to its over-representation (1 every 13 kb). This certainly would ensure the rapid encounter of a KOPS by a newly loaded FtsK ring.

KOPS stop FtsK translocation on DNA

Two different mechanisms may account for the fact that KOPS direct the orientation of FtsK translocation on DNA: KOPS

may be preferred loading sites and orient FtsK translocation at the binding step. Alternatively, translocating FtsK may be stopped, unloaded from DNA or reversed when encountering KOPS in the nonpermissive orientation. These two hypotheses are not exclusive. On the one hand, the observations that aggregates of $FtsK_{50C}$ oscillate around *dif in vitro* (Pease *et al*, 2005) and that $FtsK_{50C}$ frequently reverts its direction of translocation when encountering KOPS (Figure 5) argue towards a mechanism independent of loading. However, it is not obvious from these data whether it is the same FtsK motor that translocates in both directions. On the other hand, KOPS are not strictly required for loading since FtsK may load on and translocate all DNA tested so far, some of which are devoid of GGGNAGGG motifs (Aussel *et al*, 2002; Massey *et al*, 2004; Saleh *et al*, 2004; data not shown). Taken together, these data suggest that KOPS act during FtsK translocation but do not exclude a role at the loading step.

KOPS participate in replichore organization

Bacterial chromosomes contain a single replication origin. This is most often accompanied by the presence of replichores, a term that accounts for an important bias in the sequence from the replication origin to the terminus or telomers in the case of linear chromosomes (Blattner *et al*, 1997). Skewed orientation of numerous sequence motifs participates in replichores (Blattner *et al*, 1997; Salzberg *et al*, 1998; Lobry and Louarn, 2003). Replichore organization is postulated to play roles in various DNA processing activities. Our report provides a first molecular basis for a long postulated role of an *oriC–dif* bipolar organization in chromosome structure and segregation (Rebollo *et al*, 1988). Indeed, the over-representation in the *E. coli* genome of the GGGNAGGG motif (Table II) suggests that they have been selected for their activity during evolution and reinforces the view that they are important players in chromosome organization and chromosome dynamics. Interestingly, recent data suggest that the two replichores of the *E. coli* chromosome are sequestered one from the other during chromosome segregation and each segregate to one edge of the forming sister nucleoids (Wang *et al*, 2005). This lends further support to a role of replichores in segregation.

The effect of alterations of chromosome polarity on the cell cycle implies that KOPS could participate in constraining chromosome rearrangements to conserve a global replichore organization (Eisen *et al*, 2000). Newly acquired DNA could also be counter-selected if it carries misoriented KOPS or other active signals, which may help to conserve the replichore organization. Finally, it is tempting to speculate that KOPS, or other DNA motifs, play a role in other DNA processes, such as replication, postreplicational rebuilding of nucleoid structure or compaction.

Materials and methods

Strain, plasmids and proteins

Strains were derived from LN2772 ($\Delta(dif)_{58}$::Tc; Cornet *et al*, 1994). This strain was first rendered $\Delta(dif)_{58}$::*Bam*HI using plasmid pFC15 (Cornet *et al*, 1994). A tetracycline resistance determinant (Tc) was then inserted at position *zdd355* by P1 transduction from strain LN3124 (Cornet *et al*, 1996) to yield strain FC53 (Figure 1A). Insertions of the *psi* core sequence were constructed in FC53 using plasmids derived from pLN135 (Cornet *et al*, 1996) following the general procedure described for this family of transgenesis vectors (Cornet *et al*, 1994). Briefly, this vector is thermosensitive for its replication, allowing selection of its integration into the chromosome by a first homologous recombination event, and carries the *rpsL* gene, allowing selection for its lost after excision from the chromosome by a second recombination event. Strains were screened for tetracycline sensitivity after the plasmid excision step and verified by PCR amplification and sequencing. Plasmids used for transgenesis were obtained by inserting the previously reported *Mlu*I–*psi*–*Bgl*II fragment (Capiaux *et al*, 2002) between relevant chromosomal fragments amplified by PCR (Figure 1A). To obtain the *in vitro* Xer recombination long linear substrates, plasmids were constructed by inserting KOPS-containing annealed oligonucleotides (Figure 3) as *Bgl*II–*Spe*I fragments into pFX315 (Massey *et al*, 2004). $FtsK_{50C}$ proteins were purified as described previously (Aussel *et al*, 2002). XerC and XerD were a kind gift from DJ Sherratt.

Measurement of dimer resolution activity

CDR activities were measured using the coculture assay (Perals *et al*, 2000). This assay measures the selective growth advantage of a strain compared with a $\Delta(dif)$ strain in which 15% of the cells carry unresolved chromosome dimers and thus do not form viable progeny. Strains to analyse (Tc^S) were cocultivated with LN2772 ($\Delta(dif)_{58}$::Tc). Briefly, A 1:1 mixture of the two strains was grown in serial culture in L broth at 37°C and their relative frequencies were measured by plating every 20 generations. The CDR activity (Figure 1B and Table I) was deduced from the slope of the ratio of the total number of bacteria to the number of Tc^R bacteria as a function of the number of generations. This activity is standardized as 100% for a wild-type strain and 0% for a $\Delta(dif)$ strain.

Xer recombination assay

Recombination assays were performed as described previously (Massey *et al*, 2004). Briefly, the unlabelled fragments were produced by *Nde*I–*Mlu*I restriction digestion of plasmids derived from pFX315. The short *dif*-containing labelled fragment was produced by annealing synthetic oligonucleotides, labelled at the 5′ end of the strand cleaved by XerC using T4 DNA kinase and [γ-^{33}P]ATP and purified using a MicroSpin™ G-25 column (Amersham Biosciences). Reactions were incubated at 37°C for 60 min. Reaction products were analysed by 7% TBE–PAGE and quantified using a Fuji PhosphorImager and ImageGauge software.

Preparation of substrates for T-dissociation assay

T-shaped substrates were produced in two separate steps. Two partially complementary oligonucleotides, one 51-mer (5′-ACCATGCTCGTGATTACGATATCGATGCATGCGAATTCGAGCTCGGTAC-3′) and one 55-mer (5′P-CCGAGATACCGAGCTCGAATTCGCATGCATCGATATAATACGTGAGGCCTAGGATC), were annealed to form a duplex DNA with 20 bp noncomplementary at one extremity and 4 bp protruding at the 5′ of the other extremity that allows ligation with an *Ava*I-digested fragment. To obtain the KOPS-containing long arm, the *Bgl*II–*dif*–*Mlu*I fragment of the relevant pFX315 derivatives was replaced by a *Bgl*II–*Ava*I–*Mlu*I linker. *Ava*I–*Nde*I fragments were then purified from these plasmids and ligated with the T-shaped form. The ligation product was then gel-purified using standard procedures and annealed with a ^{32}P-labelled 40-mer oligonucleotide (5′-GATCCTAGGCCTCACGTATTCTCGTAATCACGAGCATGGT-3′) complementary to the two single-stranded extremities of the duplex. Annealing was performed at 37°C for 30 min in a mixture containing 25 mM Tris-acetate (pH 8.0), 10 mM $MgAc_2$, 0.2 mM DTT and 100 μg/ml casein. The annealed substrate was purified on MicroSpin™ S-400 columns (Amersham Biosciences) pre-equilibrated with 50 mM NaCl and used immediately for the reaction.

T-dissociation assay

T-dissociation reactions (10 μl final volume) were performed in the same buffer as the annealing reactions supplemented with 1 mM ATP, 2 μl T-shaped substrates and ~250 nM of $FtsK_{50C}$ (monomer concentration). Reactions were incubated at 37°C and stopped by the addition of 2 μl of stop solution (1 mg/ml proteinase K, 1.25% SDS, 10 mM Tris–HCl (pH 7.5), 30% glycerol, 0.06% bromophenol blue, 0.06% xylene cyanol) and an excess of unlabelled 40-mer oligonucleotides. Reaction products were analysed on 7% native TBE–PAGE and quantified using a Fuji PhosphorImager and ImageGauge software.

Single molecule experiments

Experiments were performed as previously described (Saleh *et al*, 2004, 2005). Briefly, DNA substrates were obtained by restriction of plasmids and ligated to biotin- and digoxigenin-modified DNA fragments prepared by PCR using cognate modified nucleotides. The resulting constructs were incubated with 1 μm diameter paramagnetic streptavidin beads and added to 1 mm^2 cross-section glass capillaries, which had been washed with 0.1 M NaOH, coated with SigmaCote and sequentially incubated with solutions of anti-digoxigenin and bovine serum albumin. We controlled that the beads used were bound to the capillary by a single nicked DNA molecule, as described previously (Strick *et al*, 1996, 1998). Experiments were performed in a buffer containing 10 mM $MgCl_2$, 10 mM Tris pH 7.9, 50 mM NaCl, 1 mM DTT, 0.01% Triton X-100 and ATP. Protein is added by pipetting 1–3 μl of 1 μM $FtsK_{50C}$ monomers into 200 μl of buffer of the capillary, and gently mixing to reach a final concentration of 5–15 nM $FtsK_{50C}$ monomers. Typically, a single protein addition causes good activity for 30–60 min; further protein is added as necessary to maintain activity. We define 'good activity' to occur when translocation events are well separated, that is, when the typical waiting time between events is longer than the time scale of an individual event. In that limit, we can assume that a single protein complex is active (Saleh *et al*, 2004).

Immediate addition of excessive amounts of protein (more than ~30 nM $FtsK_{50C}$ monomers) consistently results in excessive activity in which individual events are no longer separated, and the bead height decreases, without return to the full baseline length, through a random sequence of increasing and decreasing translocation events (Supplementary Figure 1). This type of data is quite similar to the data taken at 100 nM $FtsK_{50C}$ shown in Figure 1B of Pease *et al* (2005). Owing to the high probability that multiple protein complexes are active, these data cannot be meaningfully interpreted in terms of the position or speed of a single FtsK motor in our system.

Statistical tests

To test whether a motif is significantly biased on one strand or not, a statistical likelihood ratio test was developed that takes into account the asymmetric oligonucleotide composition of leading and lagging strands (S Schbath and S Robin, personal communication). For this, we used a maximal Markov chain model. For instance, the S-skew (Score of skew) of an 8 bp motif is calculated taking the monomer to 7-mer composition of the chromosome into account (calculated using the R'MES package, http://www-mig.jouy.inra.fr/ssb/rmes/). An S-skew greater than 3.84 (3.84 is the 95% quantile of the $\chi^2(1)$ distribution) means that the skew is significant at a 5% level.

The over-representation of motifs was assessed as described previously (Sourice *et al*, 1998) using a maximal Markov chain model and a Gaussian approximation in the R'MES package (http://www-mig.jouy.inra.fr/ssb/rmes/). A statistical score (referred to as the score of occurrence (S-occ) in Table II) was obtained. An S-occ $\geqslant 5$ indicates that the probability that the observed occurrence is random is $\leqslant 10^{-7}$.

Supplementary data

Supplementary data are available at *The EMBO Journal* Online.

Acknowledgements

We thank J-M Louarn for helpful discussions, M Chandler and S Kennedy for critical reading, S Schbath and S Robin for the development of the statistical tests and P Lebourgeois for technical support. S Bigot and C Lesterlin were supported by MENESR studentships. O. Saleh received a Molswitch European program fellowship. Research was supported by grants from the CNRS ATIP program, from the French research ministry Fundamental microbiology and Reactional dynamics of biological systems ACI programs, from the Young researcher ACI program and from the FRM foundation for medical research.

References

Aussel L, Barre FX, Aroyo M, Stasiak A, Stasiak AZ, Sherratt D (2002) FtsK is a DNA motor protein that activates chromosome dimer resolution by switching the catalytic state of the XerC and XerD recombinases. *Cell* **108:** 195–205

Bigot S, Corre J, Louarn J, Cornet F, Barre FX (2004) FtsK activities in Xer recombination, DNA mobilization and cell division involve overlapping and separate domains of the protein. *Mol Microbiol* **54:** 876–886

Blattner FR, Plunkett III G, Bloch CA, Perna NT, Burland V, Riley M, Collado-Vides J, Glasner JD, Rode CK, Mayhew GF, Gregor J, Davis NW, Kirkpatrick HA, Goeden MA, Rose DJ, Mau B, Shao Y (1997) The complete genome sequence of *Escherichia coli* K-12. *Science* **277:** 1453–1474

Bouchiat C, Wang MD, Allemand J, Strick T, Block SM, Croquette V (1999) Estimating the persistence length of a worm-like chain molecule from force–extension measurements. *Biophys J* **76:** 409–413

Capiaux H, Lesterlin C, Perals K, Louarn JM, Cornet F (2002) A dual role for the FtsK protein in *Escherichia coli* chromosome segregation. *EMBO Rep* **3:** 532–536

Cornet F, Louarn J, Patte J, Louarn JM (1996) Restriction of the activity of the recombination site *dif* to a small zone of the *Escherichia coli* chromosome. *Genes Dev* **10:** 1152–1161

Cornet F, Mortier I, Patte J, Louarn JM (1994) Plasmid pSC101 harbors a recombination site, *psi*, which is able to resolve plasmid multimers and to substitute for the analogous chromosomal *Escherichia coli* site *dif*. *J Bacteriol* **176:** 3188–3195

Corre J, Louarn JM (2002) Evidence from terminal recombination gradients that FtsK uses replichore polarity to control chromosome terminus positioning at division in *Escherichia coli*. *J Bacteriol* **184:** 3801–3807

Corre J, Patte J, Louarn JM (2000) Prophage lambda induces terminal recombination in *Escherichia coli* by inhibiting chromosome dimer resolution. An orientation-dependent *cis*-effect lending support to bipolarization of the terminus. *Genetics* **154:** 39–48

Dixon DA, Kowalczykowski SC (1995) Role of the *Escherichia coli* recombination hotspot, chi, in RecABCD-dependent homologous pairing. *J Biol Chem* **270:** 16360–16370

Dohoney KM, Gelles J (2001) Chi-sequence recognition and DNA translocation by single RecBCD helicase/nuclease molecules. *Nature* **409:** 370–374

Eisen JA, Heidelberg JF, White O, Salzberg SL (2000) Evidences for symmetric chromosomal inversions around the replication origin in bacteria. *Genome Biol* **1** research0011.1–0011.9

El Karoui M, Biaudet V, Schbath S, Gruss A (1999) Characteristics of Chi distribution on different bacterial genomes. *Res Microbiol* **150:** 579–587

Errington J, Bath J, Wu LJ (2001) DNA transport in bacteria. *Nat Rev Mol Cell Biol* **2:** 538–545

Hendricks EC, Szerlong H, Hill T, Kuempel P (2000) Cell division, guillotining of dimer chromosomes and SOS induction in resolution mutants (*dif*, *xerC* and *xerD*) of *Escherichia coli*. *Mol Microbiol* **36:** 973–981

Hill TM (1992) Arrest of bacterial DNA replication. *Annu Rev Microbiol* **46:** 603–633

Hill TM, Marians KJ (1990) *Escherichia coli* Tus protein acts to arrest the progression of DNA replication forks *in vitro*. *Proc Natl Acad Sci USA* **87:** 2481–2485

Ip SC, Bregu M, Barre FX, Sherratt DJ (2003) Decatenation of DNA circles by FtsK-dependent Xer site-specific recombination. *EMBO J* **22:** 6399–6407

Kamada K, Horiuchi T, Ohsumi K, Shimamoto N, Morikawa K (1996) Structure of a replication-terminator protein complexed with DNA. *Nature* **383:** 598–603

Kaplan DL, O'Donnell M (2004) Twin DNA pumps of a hexameric helicase provide power to simultaneously melt two duplexes. *Mol Cell* **15:** 453–465

Kuempel P, Hogaard A, Nielsen M, Nagappan O, Tecklenburg M (1996) Use of a transposon (Tn*dif*) to obtain suppressing and nonsuppressing insertions of the *dif* resolvase site of *Escherichia coli*. *Genes Dev* **10:** 1162–1171

Lesterlin C, Barre FX, Cornet F (2004) Genetic recombination and the cell cycle: what we have learned from chromosome dimers. *Mol Microbiol* **54:** 1151–1160

Lesterlin C, Mercier R, Boccard F, Barre FX, Cornet F (2005) Roles for replichores and macrodomains in segregation of the *Escherichia coli* chromosome. *EMBO Rep* **6:** 557–562

Lobry JR, Louarn JM (2003) Polarisation of prokaryotic chromosomes. *Curr Opin Microbiol* **6:** 101–108

Massey TH, Aussel L, Barre F-X, Sherratt DJ (2004) Asymmetric activation of Xer site-specific recombination by FtsK. *EMBO Rep* **5:** 399–404

Pease PJ, Levy O, Cost GJ, Gore J, Ptacin JL, Sherratt D, Bustamante C, Cozzarelli NR (2005) Sequence-directed DNA translocation by purified FtsK. *Science* **307:** 586–590

Perals K, Cornet F, Merlet Y, Delon I, Louarn JM (2000) Functional polarization of the *Escherichia coli* chromosome terminus: the *dif* site acts in chromosome dimer resolution only when located between long stretches of opposite polarity. *Mol Microbiol* **36:** 33–43

Rebollo J, Francois V, Louarn J (1988) Detection and possible role of two large nondivisible zones on the *Escherichia coli* chromosome. *proc Natl Acad Sci USA* **85:** 9391–9395

Saleh OA, Bigot S, Barre FX, Allemand JF (2005) Analysis of DNA supercoil induction by FtsK indicates translocation without groove-tracking. *Nat Struct Mol Biol* **12:** 436–440

Saleh OA, Perals C, Barre FX, Allemand JF (2004) Fast, DNA-sequence independent translocation by FtsK in a single-molecule experiment. *EMBO J* **23:** 2430–2439

Salzberg SL, Salzberg AJ, Kerlavage AR, Tomb JF (1998) Skewed oligomers and origins of replication. *Gene* **217:** 57–67

Sharp MD, Pogliano K (2002) Role of cell-specific SpoIIIE assembly in polarity of DNA transfer. *Science* **295:** 137–139

Sourice S, Biaudet V, El Karoui M, Ehrlich SD, Gruss A (1998) Identification of the Chi site of *Haemophilus influenzae* as several sequences related to the *Escherichia coli* Chi site. *Mol Microbiol* **27:** 1021–1029

Spies M, Bianco PR, Dillingham MS, Handa N, Baskin RJ, Kowalczykowski SC (2003) A molecular throttle: the recombination hotspot chi controls DNA translocation by the RecBCD helicase. *Cell* **114:** 647–654

Strick TR, Allemand JF, Bensimon D, Bensimon A, Croquette V (1996) The elasticity of a single supercoiled DNA molecule. *Science* **271:** 1835–1837

Strick TR, Allemand JF, Bensimon D, Croquette V (1998) Behavior of supercoiled DNA. *Biophys J* **74:** 2016–2028

Taylor AF, Schultz DW, Ponticelli AS, Smith GR (1985) RecBC enzyme nicking at Chi sites during DNA unwinding: location and orientation-dependence of the cutting. *Cell* **41:** 153–163

Wang X, Possoz C, Sherratt DJ (2005) Dancing around the divisome: asymmetric chromosome segregation in *Escherichia coli*. *Genes Dev* **19**, in press

Yates J, Aroyo M, Sherratt DJ, Barre FX (2003) Species specificity in the activation of Xer recombination at dif by FtsK. *Mol Microbiol* **49:** 241–249

